This is NPRs compilation, and current understanding of, the emails and discussions that went back in forth first in late July, and then moreover around the 10th August and the first week in September.

The basic picture is outlined below and given in Figure 1.

1. We start with an inflated disk, with non-zero torque at the ISCO, and $h/R \sim 0.2$ inside of $R \sim 100R_{\rm g}$. This is the initial state in circa 2000.

2. 'Something' happens, around 2007, to provoke a switch to a zero torque at ISCO state.

   There are two basic scenarios to this 'something':. First, this could is likely due to going from a nonzero torque (NZT) condition at the inner boundary of the disk to a zero torque (ZT) condition. This could be triggered by a B-field collapse, contraction or ejection close to the BH. Alternatively, using the "Lamppost model" of AGN coronae, the lamppost is being raised so there is less heating of the inner disk and the cooling front propagates outwards.

3. A cooling front is set-up, which propagates out from the ISCO at the timescale, $t_{\rm front}$. Regions behind the front emit flux at 0.1 of what they did prior to the passage of the front (due to drop in T? T $\downarrow \times 1.78 \Rightarrow L \downarrow \times 10$) , and the temperature decrease leads the height to drop by a factor of 2 (just due to less kinetic energy??). $L_{\rm ion}$ starts dropping due to the drop in ionizing photons, which in turn causes the H-lines to also start to drop.

4. Because the disk starts fat, the cooling front time is not that long, and by 2010 (3 years later), the front has reached $R \sim 50R_g$. During that time, the collapsing disk height increases the number density of scatterers, which in turn causes Rayleigh scattering producing the blue downturn in the 2010 spectrum.

5. The cooling front keeps going, until it hits the part of the disk where it is normally thin, around $R = 100R_g$, arriving around 2012. This sets up another (heating) front, which will travel *back in* towards the SMBH, and re-inflate the disk. This 'returning' front travels more slowly because the disk is thinner. It also means the return to normal will be asymmetric in time, as observed, and the g-band bottoms out first because that is coming from $R \sim 100R_g$.

6. We expect the front to return to the ISCO in about 2018. That means the H lines will come back a few months later, but the WISE IR flux shouldn't come back until about 2021.

Symbol	quantity	units	typical values
$\sum$	disk surface density		
n_e	electron density		
$n_{\rm RS}$	number density of Rayleigh scatterers		
κ	opacity		
$\kappa_{\rm es}$	electron scattering opacity		
τ	optical depth		
σ_R	Rayleigh cross-section ($\propto 1/\lambda^4$)		
$T_{\rm eff}$	effective disk surface temperature		
$T_{\rm mid}$	midplane temperature		
$\sigma_{\rm T}$	Thompson cross-section		
V_R	radial velocity	cm s^{-1}	
Ω	angular velocity	rad s^{-1}	
$R\frac{\partial\Omega}{\partial R}$	velocity shear		
ν	kinematic viscosity	cm^2 s^{-1}	

Table 1:

$$I = (2hc^2/\lambda^5)/(\exp(hc/(\lambda k_{\rm B}T)) - 1) \tag{1}$$

$$\begin{aligned} T_{\rm NZT} &= fT_{\rm SG} && (2)\\ &= fp_f\dot{m}_{\rm Edd}^{1/4}r^{-0.75} && (3)\\ &= f\left(\frac{3/2c^5m_p}{\epsilon GM_{\rm SMBH}M_\odot\sigma_{\rm T}\sigma_{\rm SB}}\right)^{1/4}\dot{m}_{\rm Edd}^{1/4}r^{-0.75} && (4)\\ & && (5)\end{aligned}$$

$$\begin{aligned} L_{\rm Edd} &= \frac{4\pi GM_{\rm BH}c}{\kappa_{\rm es}} && (6)\\ &= \frac{4\pi GM_{\rm BH}c}{\kappa_{\rm es}} && (7)\\ & && (8)\end{aligned}$$

Finally, equation (**??**) should be evaluated at the radius $R_{\rm acc}$ where accretion itself maintains stability to local gravitational perturbations, i.e., $Q \gg 1$. Inside this radius, star formation ceases, and $\dot{M} \simeq$ constant.

The value of $R_{\rm acc}$ in fact depends on the mechanism of angular momentum transport. For local angular momentum transport, $R_{\rm acc} \sim 0.01$ pc, while for larger-scale torques, $R_{\rm acc} \sim 0.1$ pc (**?**). Our calculations favor the latter physics, so we take $R_{\rm acc} \sim 0.01\,R_{\rm BH}$, which corresponds to $R_{\rm acc} \sim 0.1$ pc for typical parameters (it makes little difference, to within the scatter and accuracy of our formula, if we take $R_{\rm acc}$ to be a fixed physical radius instead).

With these assumptions we find that our analytic gravitational torque inflow model predicts a BH inflow rate of

$$\frac{\dot{M}_{\rm BH,\,grav}}{M_\odot\,{\rm yr}^{-1}} \approx \alpha(\eta_K)\,f_d^{7/6}\,(1+1.71\,f_d^{-4/3})^{-1} \left(\frac{M_{\rm BH}}{10^8\,M_\odot}\right)^{1/6} \left(\frac{M_d(R_0)}{10^9\,M_\odot}\right)^{1} \left(\frac{R_0}{100\,{\rm pc}}\right)^{-3/2} \left(\frac{R_{\rm acc}}{10^{-2}\,R_{\rm BH}}\right)^{5/6} \left[1+\frac{f_0}{f_{\rm gas}(R_0)}\right]^{-1} \tag{9}$$

where $\alpha(\eta_K)$ is a dimensionless constant discussed below. In a simpler form, equation 9 becomes

$$\frac{\dot{M}_{\rm BH,\,grav}}{M_\odot\,{\rm yr}^{-1}} \approx \alpha(\eta_K)\,f_d^{5/2}\,M_{\rm BH,\,8}^{1/6}\,M_{d,\,9}\,R_{0,\,100}^{-3/2}\,(1+f_0/f_{\rm gas})^{-1} \tag{10}$$

$$\dot{M}_{\rm torque} \propto e_{\rm T}\,f_d^{5/2}\,M_d\,R_0^{-3/2}\,M_{\rm BH}^{1/6} \tag{11}$$

with

$$f_0 \approx 0.31\,f_d^2\left(\frac{M_d(R_0)}{10^9\,M_\odot}\right)^{-1/3} \tag{12}$$

$$f_{\rm gas}(R_0) \equiv M_{\rm gas}(R_0)/M_d(R_0) \tag{13}$$

Recall that f_d in equations 9 and 10 is the total (stellar and gas) disk mass fraction evaluated at R_0. Note also that these predictions for $\dot{M}_{\rm BH,\,grav}$ can, under a variety of circumstances, exceed the Eddington accretion rate. How much above Eddington the BH can in fact accrete depends on the uncertain physics of radiation-pressure dominated, super-Eddington accretion; much of the mass may in fact be unbound at radii smaller than we consider here. This is less likely to be a concern for $\dot{M}_{\rm BH,\,grav} \lesssim \dot{M}_{\rm Edd}$.

Despite the complex expressions leading to the final result for $\dot{M}_{\rm BH,grav}$, the power-law exponents in equations 9 and 10 are reasonably insensitive to the values of η_d and η_K over the plausible range ($0 \lesssim \eta_d \lesssim 1$, $1.4 \lesssim \eta_K \lesssim 1.75$). The normalization, however, is fairly sensitive, especially to η_K, ranging from $\approx 1\,M_\odot$ yr to $\approx 18\,M_\odot$ yr for $\eta_K = 7/4$ to $3/2$, respectively (for $\eta_d = 1/2$). This is one reason why we explicitly include the constant $\alpha(\eta_K) \sim 1-10$ in equations 9 and 10. The dependence on η_K is due to the

fact that a larger η_K implies a higher star formation rate in dense gas and thus a lower BH inflow rate. Star formation on the small scales of interest here is uncertain – we choose to parameterize that in α so that the model has the advantage that it can be rescaled in a straightforward manner for many different models of star formation (via an appropriate choice of η_K or t_K). We have also made the over-simplified assumption of just one mode at each scale, when the real behavior reflects a sum over a mode spectrum; this does not change the dimensional scalings, but does enter the normalization α. The exact values we adopt here are therefore unlikely to be universally valid, but are convenient, observationally motivated, and match the choice in most of our simulations.

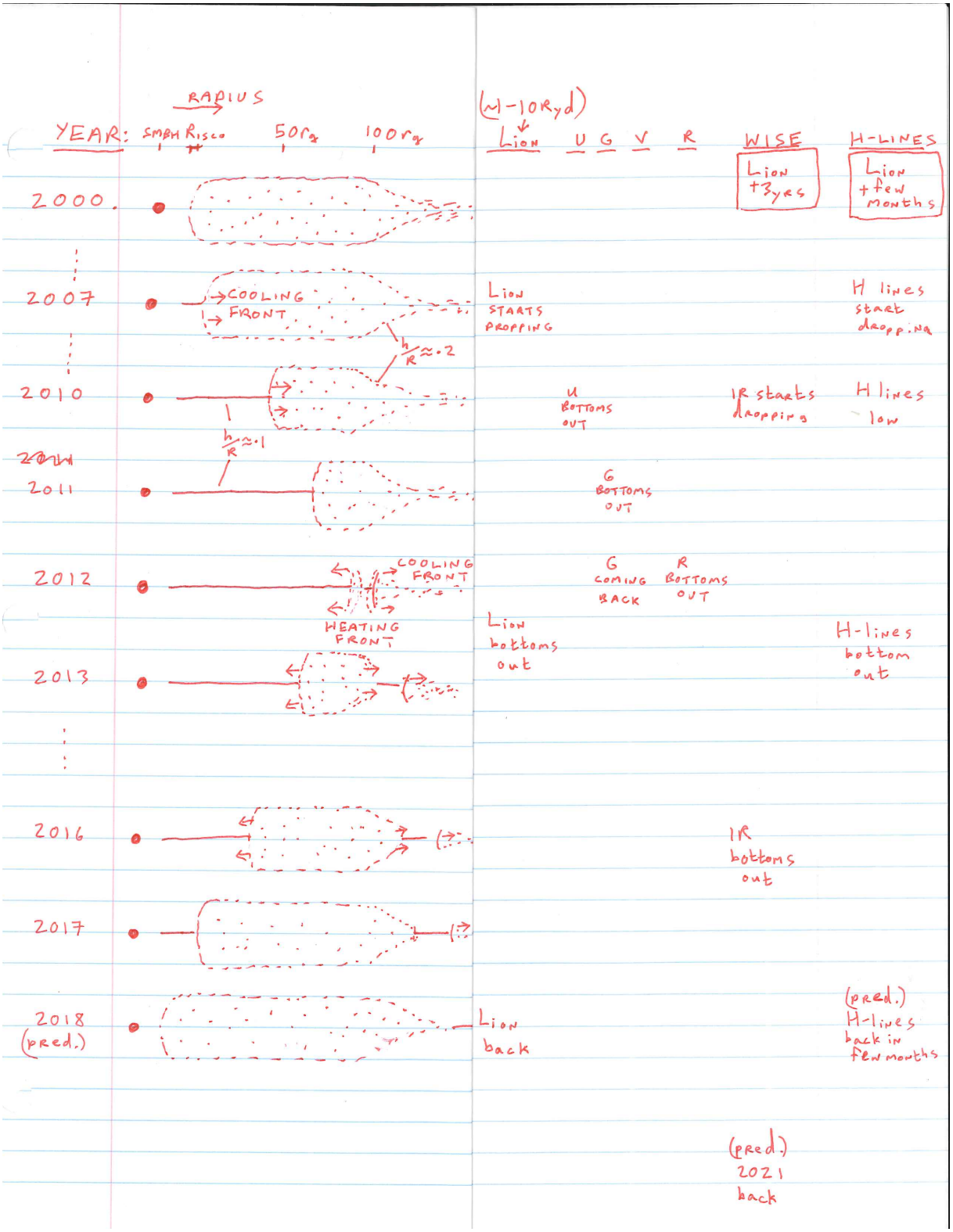

Figure 1: Our working model explaining the optical and IR light-curves, the change seen in the 3 spectra, and making predictions to what will be seen in 2018 and 2021.